

# Gesture Controlled Driving

Ollie Peng, Manish Raghavan, Victor Sutardja  
Video Demonstration: <http://www.youtube.com>

## Overview

Using the Kobuki platform from lab, we built a system by which the Kobuki drives in a path drawn by the user. Specifically, the user draws a path in the air using a brightly colored object. The Kobuki takes a series of images of this path using a webcam mounted on its frame. These images are streamed to a laptop which performs the image-processing needed to detect the object used for drawing. The points from the images are interpolated into a smooth path. Using feedback from the OptiTrack camera system, the Kobuki is instructed to drive along this path, correcting for any errors in real time.

## Setup

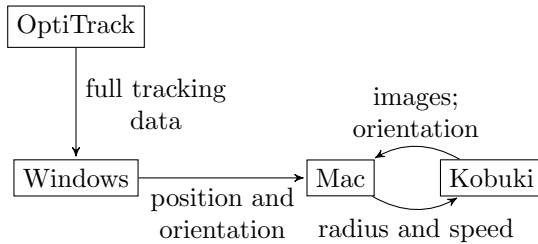


Figure 1: Flow of information

Figure 1 shows the flow of information between various devices. There are two key design decisions we made in order to overcome challenges we faced. First, we streamed the OptiTrack data to a separate Windows machine instead of the Mac that was communicating with the data because the frame rate from the tracking system was too high and would be constantly modifying shared variables. Since we were only sending updated commands to the Kobuki once every second, we did not need such frequent information, and therefore used the Windows machine to sample the data at a lower rate before passing it on the Mac. Second, we chose to take orientation data from both the OptiTrack and Kobuki. We did so because the orientation from OptiTrack was given in terms of quaternions in a rotated axis space, meaning that the standard equations for converting to yaw, pitch, and roll no longer applied. Instead, we needed to know which quadrant the yaw was in to correct them. As a result, we used the orientation from the Kobuki to determine which quadrant it was facing, allowing us to use the correct equations to get the true orientation.

## Image Processing

The first step to converting the drawn gesture to some sort of path is to capture key points along the gesture's trajectory. We set up a simple LabVIEW system to take a series of RGB pictures using the color camera attached to the myRIO. For each picture, we then apply a color threshold to mask out areas of the image with the wrong color. This leaves us with one or more contours of the correct color in our image. We can then construct a list of these contours and then iterate over the list to find the largest such contour, which will almost always correspond to the object we are trying to track. Since we want each image to identify just a single point on the path, we turn to the centroid  $(\bar{x}, \bar{y})$ , the arithmetic mean position of all points within the contour  $P$ , which we calculate using moments of the contour: [2]

$$(\bar{x}, \bar{y}) = \left( \frac{m_{10}}{m_{11}}, \frac{m_{01}}{m_{00}} \right)$$

where

$$m_{ij} = \sum_{\mathbf{p} \in P} \mathbf{p} \cdot x^i \cdot y^j$$

With all the images processed, this gives us an ordered list of  $(x, y)$  coordinates that quite accurately represent the complete gesture.

In Figure 2, the color thresholding identifies two main point clouds: the actual object and the controller's face. However, by identifying the contours of these clouds, we detect the larger of the two clouds and find the centroid of that, making our detection resilient to noisy images.

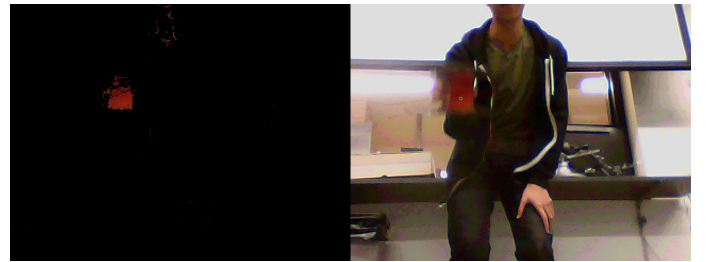


Figure 2: Detecting an object

## B-spline Interpolation

We chose B-spline interpolation with cubic polynomials because it has the following properties: [1]

- Locality – only nearest 4 points affect the curve

- Continuity – continuous up to the second derivative despite being piecewise defined system of equations:

B-spline interpolation yields a smooth path, allowing the Kobuki to drive without stopping to turn. Intuitively, the interpolation yields a path that is at any time a linear combination of three neighboring points, weighted by the basis curves at those points. Since the basis curves, shown in Figure 3 approximate Gaussians in the middle of the path (i.e. the curve shown in light blue), the interpolation can be viewed as letting each control point have “influence” on the interpolated curve that depends on how close the curve is to that point. However, this means that the interpolated curve does not actually pass through the control points. As a result, we had to take in a series of data points and find control points such that the resultant curve interpolated through the control points passes through the original data points. Figure 4 shows how from the original data points, shown in blue, a series of control points, shown in red, are computed, and when interpolated, the final path passes through the data points.

By convention, we will assume that we have  $n + 1$  data points  $\mathbf{D}_0, \dots, \mathbf{D}_n$ . To ensure that the endpoints of the curve are correct, we define

$$t_i = \begin{cases} 0 & 0 \leq i \leq 3 \\ i - 3 & 3 \leq i \leq n + 3 \\ n + 3 & n + 3 \leq i \leq n + 6 \end{cases}$$

The equations for the basis functions are given by the following recurrence relation: [3]

$$N_{i,1}(x) := \begin{cases} 1 & \text{if } t_i \leq x < t_{i+1} \\ 0 & \text{otherwise} \end{cases}$$

$$N_{i,k}(x) := \frac{x - t_i}{t_{i+k-1} - t_i} N_{i,k-1}(x) + \frac{t_{i+k} - x}{t_{i+k} - t_{i+1}} N_{i+1,k-1}(x)$$

In order to get the curve to pass through all the data points, we need 2 more control points than data points. To find the control points  $\mathbf{P}_0, \dots, \mathbf{P}_{n+2}$  from the data points, we use the fact that the curve must start and end with our first and last data points and must pass through each of our data points. Since we have  $n + 3$  control points and  $n + 1$  data points, we add the initial conditions that the second derivative of the curve at the start and end points must be 0. This yields the following

system of equations:

$$\begin{aligned} \mathbf{P}_0 &= \mathbf{D}_0 \\ \frac{3}{2}\mathbf{P}_1 - \frac{1}{2}\mathbf{P}_2 &= \mathbf{D}_0 \\ N_{i,4}(i)\mathbf{P}_i + N_{i+1,4}(i)\mathbf{P}_{i+1} + N_{i+2,4}(i)\mathbf{P}_{i+2} &= \mathbf{D}_i \\ -\frac{1}{2}\mathbf{P}_n - \frac{3}{2}\mathbf{P}_{n+1} &= \mathbf{D}_n \\ \mathbf{P}_{n+2} &= \mathbf{D}_n \end{aligned}$$

To interpolate the curve from the control points, we simply use

$$C(t) = \sum_{i=0}^{n+2} N_{i,4}(t)\mathbf{P}_i$$

Note that for any value of  $t$ , at most 4 of the  $N_{i,4}$  values are nonzero (see Figure 3), meaning the curve only depends on the nearest 4 control points.

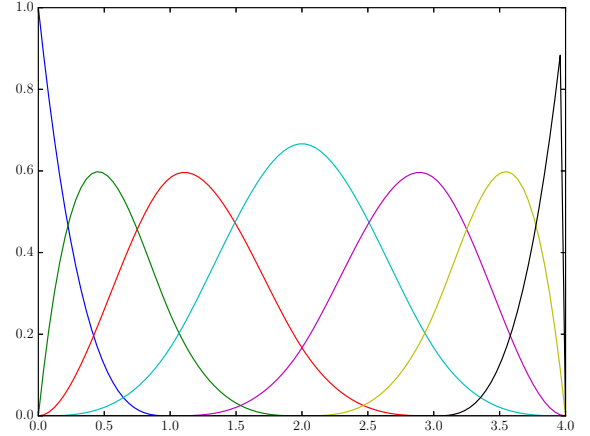


Figure 3: Cubic spline basis curves

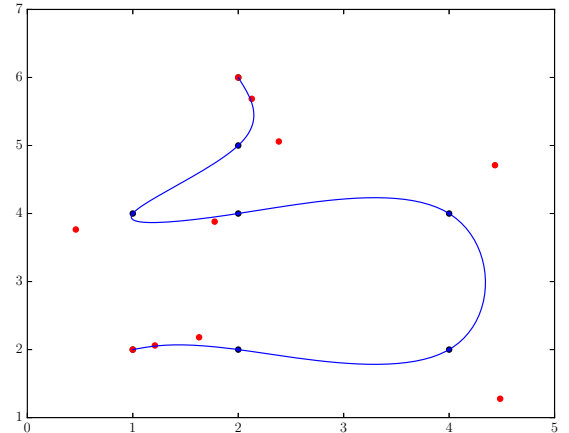


Figure 4: Sample cubic spline interpolation

## Timing

All the communication between the various systems we used had to be timed in such a way that the latency between the arrival of new data and its usage was low. The main limiting factor was that on the Kobuki, polling a socket for new data too frequently could sometimes prevent any changes in wheel speed from taking effect. In order to fix this, we made the Kobuki poll for new data every 960 ms. Data was sent by the Mac once a second, meaning the average latency between commands being issued and received was around half a second. Since the Mac was multithreaded, it polled orientation data from the Kobuki every 200 ms, meaning latency in this case was based on how frequently the Kobuki sent data (every 960 ms). Since these two were connected directly by a shared WiFi network from the Mac, the network latency was negligible compared to this. The OptiTrack frame rate was actually too high, so the Windows machine sampled every 10 frames and sent those to the Mac over a direct ethernet connection, which were then further sampled once a second. Since the frames were generated so frequently, a frame read by the Mac was in the worst case on the order of tens of milliseconds old. Overall, the latency between data being generated by OptiTrack and the Kobuki's wheel speeds being updated was in the worst case no more than around 1.2 seconds, which was sufficient to produce a path with low error.

## Threading

In controlling the Kobuki, we had to send it instructions while also receiving orientation data from it. To do so, we used threading – one thread listened for data from the Kobuki while the other thread used that data to control it. In order to prevent race conditions, we used locks on two shared resources: the socket over which we were communicating and a global variable containing the Kobuki's orientation. Since we had two threads each using the same two locks, we had to avoid deadlock, which we did by ensuring that no thread held more than one lock at the same time. Each thread executed a task periodically, on the order of tenths of a second or longer, meaning that the delay caused by waiting for locks was insignificant compared to the running time allowed for each task.

## Modeling Movement and Control

The Kobuki requires a radius of curvature and wheel speed to control its motion. Our control algorithm takes in the Kobuki's current position, the next position it should go to, its current orientation to produce these

quantities. Let  $\mathbf{p}_1 = (x_1, y_1)$  be the Kobuki's current position and  $\mathbf{p}_2 = (x_2, y_2)$  be the Kobuki's next position. Let  $\mathbf{p}_\Delta = \mathbf{p}_2 - \mathbf{p}_1$ . Let  $\phi$  be its current orientation, measured counterclockwise from the positive  $x$  axis. The angle  $\alpha$  between its current position and its next position is given by

$$\alpha = \text{sign}(y_\Delta) \arccos\left(\frac{x_\Delta}{\|\mathbf{p}_\Delta\|}\right)$$

The total angle it must turn is  $\theta = \alpha - \phi$ . The radius of curvature is then given by  $r = \frac{\|\mathbf{p}_\Delta\|}{2 \sin \theta}$ , which is positive if turning left and negative otherwise. The angle through which it must follow an arc of this circle to reach  $\mathbf{p}_2$  is  $2\theta$ , so the speed at which it must travel is  $s = \frac{2r\theta}{\tau}$ , where  $\tau$  is the time allotted for it to reach  $\mathbf{p}_2$ . Figure 5 shows the model of the Kobuki's path from  $\mathbf{p}_1$  to  $\mathbf{p}_2$ .

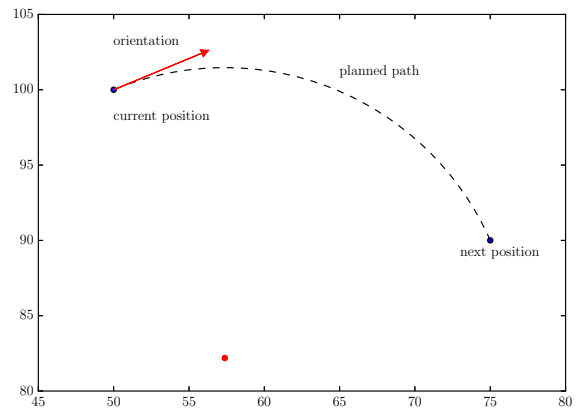


Figure 5: Movement planning

As long as  $\theta$  is small, the path produced is small and does not oscillate. However, for paths along which the radius of curvature changes drastically (meaning the third derivative of the interpolated path is high),  $\theta$  can become larger, causing the Kobuki to get off course.

## Challenges

One of the major issues we faced was communication between devices over networks we could not control. Because AirBears2 blocks traffic on some ports, we had to set up our own local networks, while remaining connected to the Internet to stream OptiTrack data. In such a complex network, new problems arose arbitrarily as factors outside our control made our communications unpredictable.

Another challenge we faced was getting the Kobuki's orientation from OptiTrack. The OptiTrack system sends

the orientation in terms of quaternions, with two major issues: the axis that OptiTrack uses is nonstandard (the  $y$  axis points up instead of  $z$ ) and every so often the system randomly perceives that the Kobuki has flipped over  $180^\circ$ , meaning the orientation suddenly becomes negative. To solve these challenges, we did the following:

1. Calculated the yaw using the standard equation for pitch: [4]

$$\theta = \arcsin(2(q_w q_y - q_x q_z))$$

2. Since  $\arcsin$  returns a result between  $-\frac{\pi}{2}$  and  $\frac{\pi}{2}$ , we took orientation data from the Kobuki as well to determine if it was facing in the positive or negative  $x$  direction, calculating the overall yaw to be  $\theta$  or  $\pi - \theta$  in the two cases respectively.

This allowed us to continue to use the more accurate OptiTrack data, only using the Kobuki's orientation to corroborate the data sent by OptiTrack.

## Results

Figures 6 and 7 depict examples of the Kobuki's actual path (shown in blue) compared to the planned path (shown in red), as tracked by the OptiTrack system.

For the path shown in Figure 6, the RMS deviation from the path is 6.074 mm. The deviation occurs because the Kobuki is always in a sense "catching up" to where it should be on the path, so it tends to cut the corners. In Figure 7, the RMS deviation rises to 14.293 mm because the radius of curvature must change much more quickly.

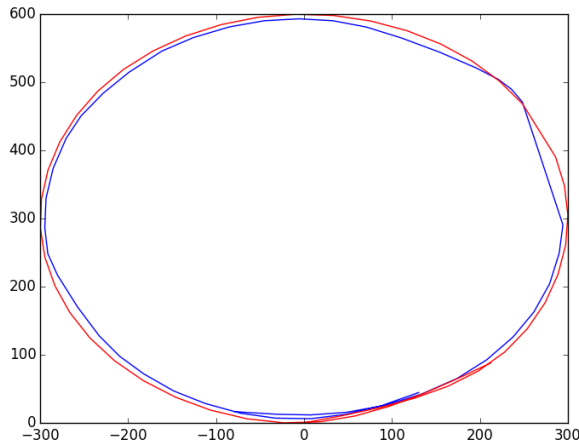


Figure 6: Actual vs. planned path with low third derivative

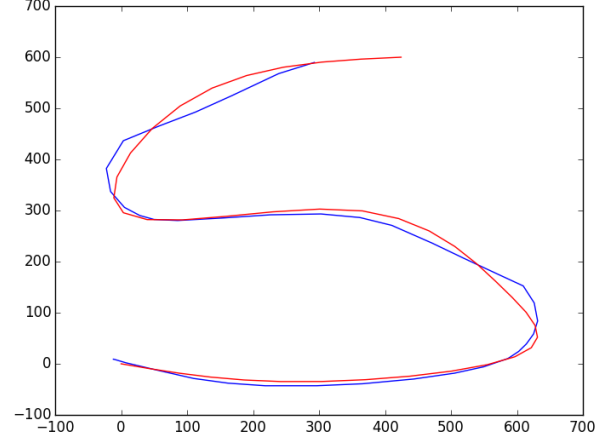


Figure 7: Actual vs. planned path with high third derivative

A video of the Kobuki following the path shown in Figure 7 can be found at <http://www.youtube.com>

## Extensions

In order to improve performance on instances with high third derivatives, we could either send commands to the Kobuki more frequently or reduce the speed at which the Kobuki follows the path. Doing either would allow us to react to deviations from the true path more quickly, thus reducing the overall error. We could also modify the control algorithm to create a plan that looks beyond just the next point – for example, we could consider the desired orientation upon reaching the next point. This would allow the planned route to better approximate the actual path, reducing error.

Since our final control algorithm only used position, next position, and orientation, it could be easily extended to allow the Kobuki to follow a moving object. As long as the Kobuki's position and orientation are sampled frequently enough, it could follow a moving object using the same techniques.

## References

- [1] Fuhua Cheng. Curve interpolation using uniform cubic b-spline curves. <http://www.cs.uky.edu/~cheng/cs631/Notes/CS631-Chap3-3.pdf>, Sep 2012. [Online; accessed 12-December-2015].
- [2] OpenCV. Structural analysis and shape descriptors — opencv 2.4.12.0 documentation. [http://docs.opencv.org/2.4/modules/imgproc/doc/structural\\_analysis\\_and\\_shape\\_descriptors.html](http://docs.opencv.org/2.4/modules/imgproc/doc/structural_analysis_and_shape_descriptors.html), 2014. [Online; accessed 12-December-2015].
- [3] Wikipedia. B-spline — Wikipedia, the free encyclopedia. <https://en.wikipedia.org/wiki/B-spline>, 2015. [Online; accessed 12-December-2015].
- [4] Wikipedia. Conversion between quaternions and euler angles — Wikipedia, the free encyclopedia. [https://en.wikipedia.org/wiki/Conversion\\_between\\_quaternions\\_and\\_Euler\\_angles](https://en.wikipedia.org/wiki/Conversion_between_quaternions_and_Euler_angles), 2015. [Online; accessed 12-December-2015].